DOI: 10.24850/j-tyca-14-05-06

Articles

Characterization of the hydrochemistry in a high Andean sub-basin in the region of Moquegua, Peru

Caracterización hidroquímica de una subcuenca altoandina en el departamento de Moquegua, Perú

Kimberly Visitación-Bustamante[1], ORCID: https://orcid.org/0000-0003-2531-413X

Lia Ramos-Fernandez[2], ORCID: https://orcid.org/0000-0003-3946-7188

Lizardo Visitación-Figueroa[3], ORCID: https://orcid.org/0000-0001-9625-2066

[1]Universidad Nacional Agraria La Molina, La Molina, Peru, kvisitacionb@gmail.com

[2]Universidad Nacional Agraria La Molina, La Molina, Peru, liarf@lamolina.edu.pe

[3]Universidad Nacional Agraria La Molina, La Molina, Peru, lvisitacion@lamolina.edu.pe

Corresponding author: Kimberly Visitación-Bustamante, kvisitacionb@gmail.com

2023, Instituto Mexicano de Tecnología del Agua. Open Access bajo la licencia CC BY-NC-SA 4.0 (https://creativecommons.org/licenses/by-nc-sa/4.0/)

Abstract

This study evaluates the hydrochemical variability of the Asana River affected by the influence of the Millune Creek in Moquegua, Peru. The water quality monitoring data from 2010 to 2018 were analyzed using Gibbs diagrams, molar ratios, Piper diagrams, Stiff diagrams, and the PHREEQC hydrogeochemical model for the identification of water saturation indices and the main minerals to which the bodies of water were exposed. Principal component analysis enabled the identification of the variability of the hydrochemistry as a function of the source and its seasonality. The results showed that the waters of Millune Creek, a tributary of the Asana River, were acidic in nature and had high concentrations of aluminum and manganese ions with respect to what was established in the ECA water (Environmental Quality Standard for Water), while the Asana River had low concentrations. Both rivers naturally have calcium sulfate. The aluminum and manganese ions were from the weathering of the mineral alunite and the erosion of the soil mineral contribution by the gradual thawing of the Arundani Mountains, which are located at the origin of the Asana River basin. Finally, the Asana River, due to its buffering capacity, neutralizes acidic waters and decreases the solubility of dissolved cations.

Keywords: Aluminum, hydrochemistry, water quality, erosion, Moquegua.

2023, Instituto Mexicano de Tecnología del Agua. Open Access bajo la licencia CC BY-NC-SA 4.0 (https://creativecommons.org/licenses/by-nc-sa/4.0/)

Resumen

El presente estudio evalúa la variabilidad hidroquímica del río Asana por influencia de la quebrada Millune en Moquegua, Perú. Se analizó la información de monitoreos de calidad de agua durante el periodo 2010-2018 a través de los diagramas de Gibbs, las relaciones molares, el diagrama de Piper, el diagrama de Stiff y el modelo hidrogeoquímico PHREEQC para la identificación de los índices de saturación de los principales minerales a los que están expuestos los cuerpos de agua en evaluación. El análisis por componentes principales permitió la identificación de la variabilidad de la hidroquímica en función de la naturaleza de la fuente y su estacionalidad. Los resultados obtenidos muestran que las aguas de la quebrada Millune, afluente del río Asana, son de naturaleza ácida con presencia de iones de aluminio y manganeso en concentraciones elevadas respecto a lo establecido en el ECA agua (estándar de calidad ambiental de agua), a diferencia del río Asana, que presenta concentraciones bajas; ambos ríos son de naturaleza sulfatada cálcica. Se determinó que los iones aluminio y manganeso se deben a la meteorización del mineral alunita y erosión del suelo, aporte mineral, por el deshielo paulatino del nevado Arundani, ubicado en la cabecera de cuenca del río Asana. Finalmente, el río Asana, por su capacidad de amortiguamiento, neutraliza las aguas ácidas y disminuye la solubilidad de los cationes disueltos.

Palabras clave: aluminio, hidroquímica, calidad del agua, erosión, Moquegua.

2023, Instituto Mexicano de Tecnología del Agua. Open Access bajo la licencia CC BY-NC-SA 4.0 (https://creativecommons.org/licenses/by-nc-sa/4.0/)

Received: 22/04/2021

Accepted: 03/15/2022

Introduction

Water is a vital and indispensable resource (Vörösmarty *et al*., 2010; Qin, Liu, Yan, & Huang, 2019) that is part of natural ecosystems, and its hydrochemical composition is influenced by natural factors, such as the hydrological cycle and climatic conditions, soil, pollution of geological origin (Hamzah, Aris, Ramli, Juahir, & Sheikhy-Narany, 2017; Devic, Djordjevic, & Sakan, 2014; De-Andrade, Palácio, Souza, De-Oliveira-Leão, & Guerreiro, 2008; Helena *et al*., 2000), anthropogenic factors and effect of climate change.

Peru, due to its mineralogical nature in the mountain system of the Andes, generates conditions that favor the dispersion of metals in waterways (Villena-Chávez, 2018). Therefore, studies on the hydrochemical variation in surface waters are necessary to provide information on environmental change, the relationships between regional chemical weathering and hydrogeochemical reactions and the mechanisms that control these relationships (Jiang *et al*., 2020).

Volcanic soils in arid zones such as Moquegua influence the chemical composition of water (Ece, Schroeder, Smilley, & Wampler, 2008; GRM, 2011; Luque-Poma, Pari-Pinto, Dueñas-Olivera, Huamán-Nieto, 2020). Likewise, the melting of glaciers can release pollutants to water bodies

2023, Instituto Mexicano de Tecnología del Agua. Open Access bajo la licencia CC BY-NC-SA 4.0 (https://creativecommons.org/licenses/by-nc-sa/4.0/)

since they expose land cover that is easily eroded by the runoff generated by the effect of thawing and the presence of steep slopes (Ban, Lei, Chen, & Liu, 2016); these soils contain various minerals, such as alunite and kaolinite (Carrino, Crosta, Toledo, Silva, & Silva, 2015), which contribute metals, such as aluminum, manganese, and iron, and anions, such as sulfates, to the water.

Millune Creek and the Asana River, tributaries of the Ilo-Moquegua River, are located in the extreme southwest of Peru in the department of Moquegua and originate from the volcanic snow-capped Arundani and Chuquiananta Mountains (GRM, 2011; ANA, 2018). Previous studies have reported the main ionic chemistry of the largest rivers in the world, such as the Amazon River (Gibbs, 1970). However, in Peru, most studies have focused on the diagnosis of compliance with environmental quality standards but not on the nature and hydrochemical variability; thus, an exhaustive analysis of the spatiotemporal variation in water quality and the environmental changes that occur in the basin is needed. For the latter, it is important to identify the mechanisms that control the composition of water and information that enables the identification of the natural or anthropogenic sources of metal contamination to water; these mechanisms can include rock weathering, precipitation, evaporation or wastewater discharge (Gibbs, 1970; Gao *et al*., 2017).

The integration of hydrochemical investigations, which involve chemical and statistical analyses, is carried out to evaluate the factors that control hydrochemistry and potential contamination (El-Alfy, Aref, Fathy, & Abdulaziz, 2017). The study of the hydrochemistry of natural

2023, Instituto Mexicano de Tecnología del Agua. Open Access bajo la licencia CC BY-NC-SA 4.0 (https://creativecommons.org/licenses/by-nc-sa/4.0/)

waters can provide important information on environmental change (Han & Liu, 2000; Gao *et al*., 2017). For this reason, identifying the factors and processes through which natural and/or human activities affect the hydrochemical variability of rivers provides a scientific basis for environmental protection, economic development and academic progress. In this study, the hydrochemical variability of the Millune Creek and the Asana River was characterized to identify the mechanisms that control the chemical composition and evaluate the influence on water quality.

Study area

The study area includes the sub basin of the Asana River (Figure 1), specifically the area of confluence of Millune Creek with the Asana River. The study area has an elevation ranging from 3 071 to 5 492 masl in the district of Torata, and it is northeast of the city of Moquegua, Peru. The upper basin of the Asana River is formed by slopes of less than 36%, with a shape factor of 0.27 and a compactness coefficient of 1.51, suggesting there is a rapid response to runoff. Meanwhile, Millune Creek has a drainage area of 23,645 km^2 and an average annual flow of 0.143 m3/s (Knight Piésold Consultores, S. A., 2008). The rocky bottom is constituted by the lithostratigraphic unit “Super Yarabamba Unit” (KsP-ya/di) and the Huaylillas Formation (Nm-hu). The region has a temperate subhumid and cold boreal climate according to the Köppen classification, with a seasonal annual rainfall amount of 243 to 460 mm/year, mainly occurring from

2023, Instituto Mexicano de Tecnología del Agua. Open Access bajo la licencia CC BY-NC-SA 4.0 (https://creativecommons.org/licenses/by-nc-sa/4.0/)

January to March (Montesinos, Cleef, & Sykora, 2012; Rau, 2017), and a dry season that spans from May to December.

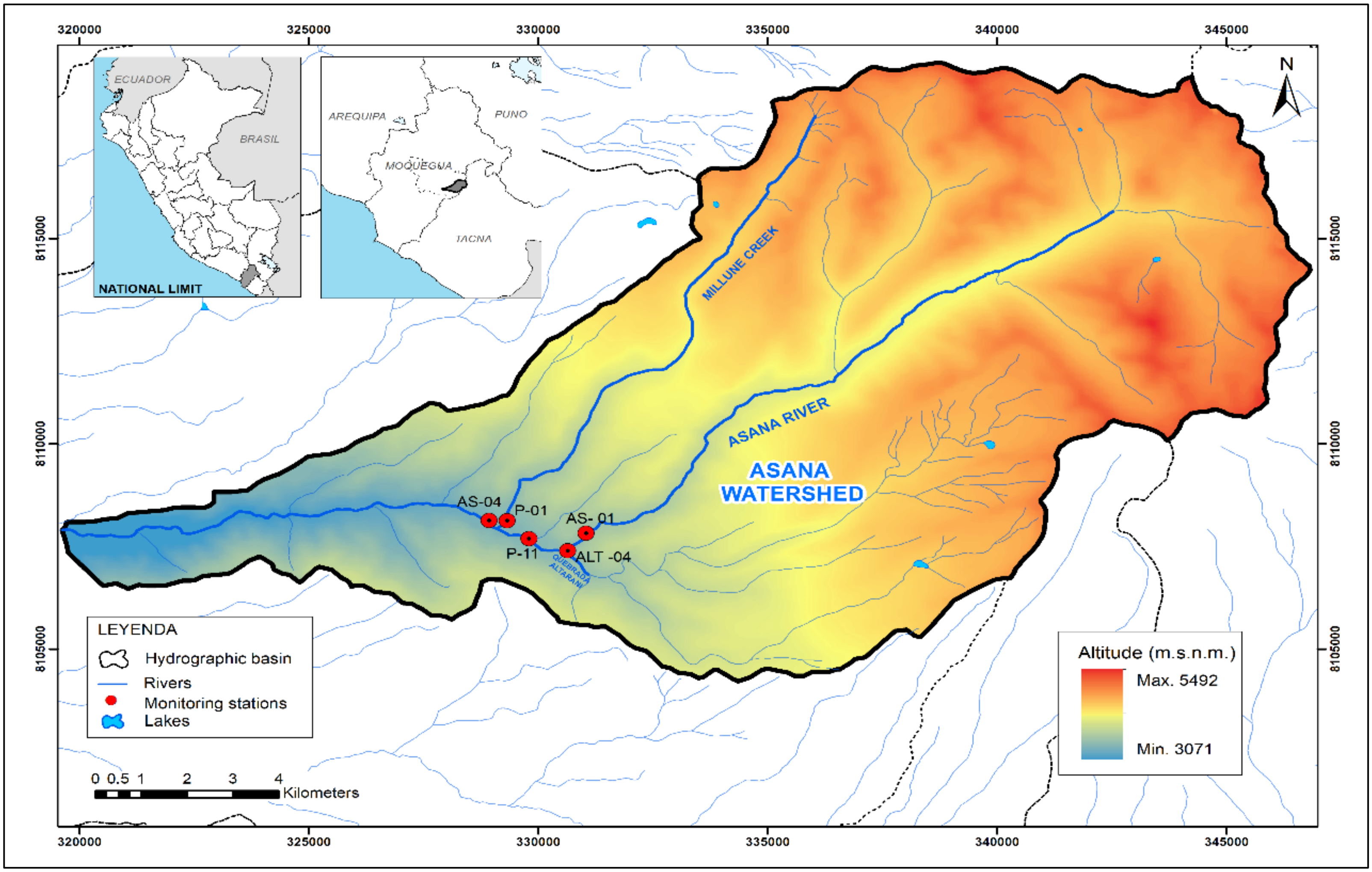

Figure 1. Location of the Asana River basin and its confluence with Millune Creek.

Materials and methods

Water quality information

The monitoring stations selected for this research were in the Asana River upstream of the confluence with the Altarani stream (AS-01), downstream of the confluence with the Altarani stream (P-11) and downstream of the confluence with Millune Creek (AS-04); additionally, we included the station in the Altarani ravine upstream confluence with the Asana River (ALT-04) and the station in the Millune ravine, which is upstream of the confluence with the Asana River (P-1). Monthly information on the physicochemical parameters was available for the period 2010-2018, in both the wet and the dry seasons.

Processes that control hydrochemistry

The determination of the processes that control hydrochemistry was evaluated using *boxplot* diagrams, Gibbs diagrams and the following molar ratios: Mg/Ca-Mg/Na, Ca/Na-Mg/Na, Ca/Na-HCO $_3$/Na, and Na-Cl (Gibbs, 1970; Gao *et al*., 2017). The hydrochemical evaluation was evaluated using the Piper diagram and the Stiff diagram (Stiff, 1951), which were plotted in the software AquaChem (Waterloo Hydrogeologic, 2020). Finally, geochemical modeling was used in the PHREEQC *software* (Parkhurst & Appelo, 1999) to identify the saturation indices that provide

2023, Instituto Mexicano de Tecnología del Agua. Open Access bajo la licencia CC BY-NC-SA 4.0 (https://creativecommons.org/licenses/by-nc-sa/4.0/)

information on the dissolution and/or precipitation of the main minerals to which the water bodies under evaluation are exposed.

Landslide susceptibility

The hydrochemical results were represented on the landslide susceptibility map (Villacorta, Fidel, & Zavala, 2012) to understand the processes that may be involved. This map expresses the degree of susceptibility at very low, low, medium, high and very high scales based on the following criteria: the presence of faults, the degree of weathering, and the presence of surface deposits and slopes (Villacorta *et al*., 2012).

Principal component analysis

Principal component analysis (PCA), a statistical type of multivariate analysis, was used to evaluate the spatial and temporal variability in water quality by correlating parameters with factors that were associated with a source or origin of the variability, such as runoff, precipitation, groundwater entry, and anthropogenic pollution (Ouyang, 2005; Jiang *et al*., 2020).

2023, Instituto Mexicano de Tecnología del Agua. Open Access bajo la licencia CC BY-NC-SA 4.0 (https://creativecommons.org/licenses/by-nc-sa/4.0/)

Results and discussion

The distribution of the results of the physicochemical parameters in the study area in the wet and dry seasons (Figure 2) confirmed that there was greater rainfall in the January-April period (wet season) due to the effects of rain compared to the rest of the year (dry season), as was historically recorded in the period 1969-1999 (Ng, Peña, & Acosta, 2019). The concentrations of dissolved oxygen had maximum values between 6.8 and 7.9 mg/l, which indicated that the main sources of water were superficial, e.g., coming from snowmelt; however, when observing the minimum values that were between 4.0 and 5.2 mg/l at stations ALT-04, AS-01, P-11 and P-1, the main sources of water would be related to the contribution of groundwater (Schreier, Erlebach, & Albright, 1980) from rock infiltrations and fractures caused by volcanoes (Ng *et al*., 2019). The pH values in the Asana River and Altarani Creek presented values between 7.1 and 7.8. Furthermore, in Millune Creek, the pH values were acidic in nature (pH 4.6) throughout the year, which was due to the low buffer capacity of the water and the dissolution of sulfated aluminum minerals such as alunite from the rocky soil of volcanic origin (Carrino *et al*., 2015); this process reduces the pH of the water by consuming hydroxyl ions and releasing sulfate and potassium ions (Acero, Hudson-Edwards, & Gale, 2015). The electrical conductivity values in the Asana River and Altarani Creek (84.8-174.6 µS/cm) were lower than those reported for Millune Creek (342.4-369.7 µS/cm). Values were higher than those of the wet season due to processes of evaporation and flow reduction, as well as the

2023, Instituto Mexicano de Tecnología del Agua. Open Access bajo la licencia CC BY-NC-SA 4.0 (https://creativecommons.org/licenses/by-nc-sa/4.0/)

greater oxidation of metals that were released from the soil (Saarinen & Kløve, 2012). Similarly, the content of total dissolved solids was higher in Millune Creek in the dry season. The total hardness in the Asana River and Altarani Creek had values between 11.4 and 54.6 mg $CaCO_3$/l due to the presence of calcium and magnesium ions in the form of bicarbonate and sulfate; however, in Millune Creek, the highest values of total hardness varied from 94.0 to 98.7 mg $CaCO_3$/l, especially in the dry season, which was possibly due to the presence of calcium and magnesium in the form of sulfate from the dissolution of sulfated minerals such as alunite or jarosite (Acero *et al*., 2015).

2023, Instituto Mexicano de Tecnología del Agua. Open Access bajo la licencia CC BY-NC-SA 4.0 (https://creativecommons.org/licenses/by-nc-sa/4.0/)

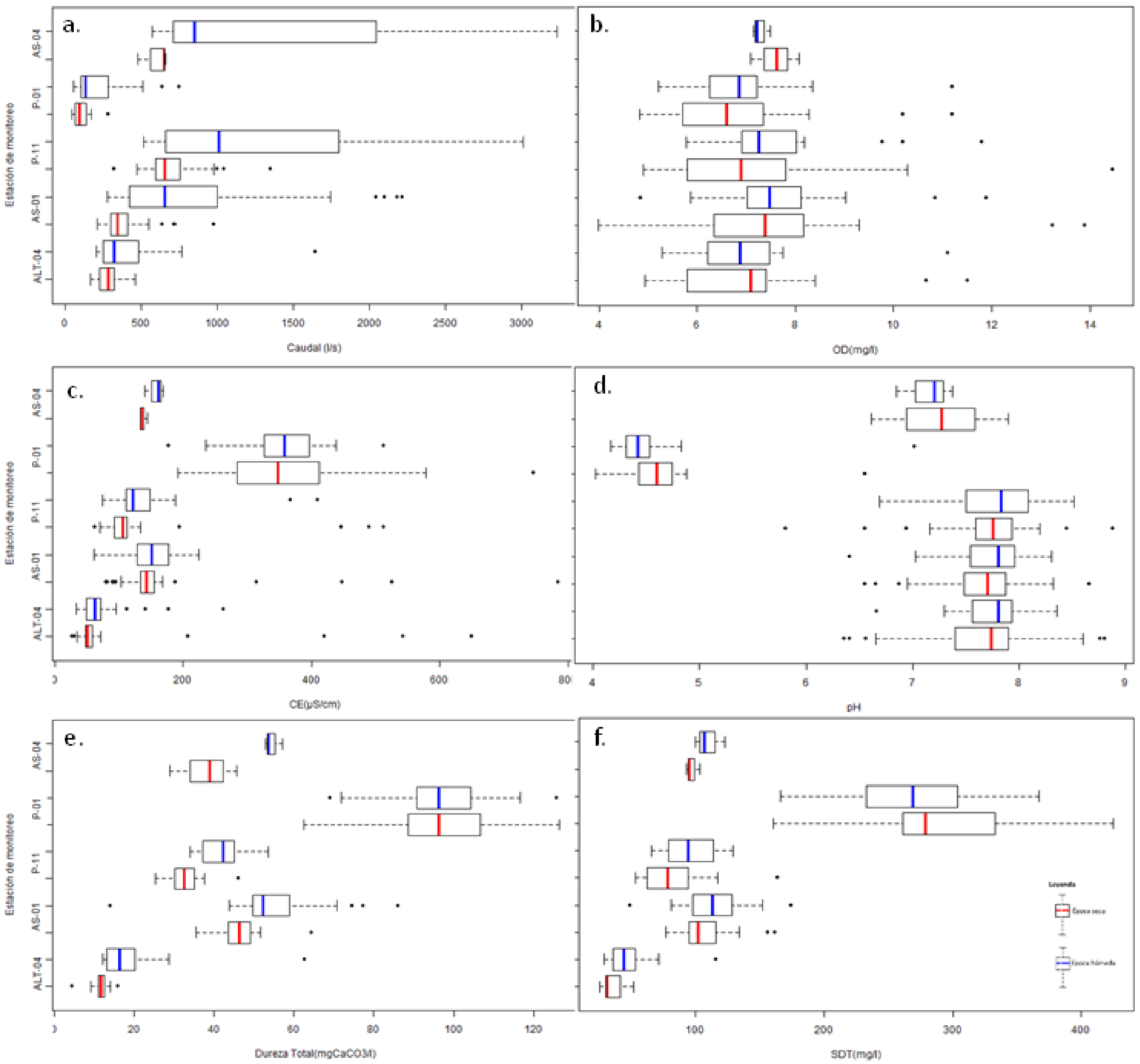

Figure 2. Boxplot diagram of the physicochemical parameters of water quality in wet and dry seasons: flow rate (a); dissolved oxygen (b); electrical conductivity (c); pH (d), total hardness (e), and dissolved solids total (f) of the Asana (AS-01 and P-11), Altarani (ALT-04) and Millune (P-1) Rivers.

2023, Instituto Mexicano de Tecnología del Agua. Open Access bajo la licencia CC BY-NC-SA 4.0 (https://creativecommons.org/licenses/by-nc-sa/4.0/)

In general, the analysis of cations and anions is performed with calcium, magnesium, sodium and potassium cations, as well as with bicarbonate, sulfate and chloride anions (Thomas, Joseph, & Thrivikramji, 2015; Gao *et al*., 2017). In our study, to reduce the error in the ionic balance, aluminum, iron and manganese were additionally considered as major cations due to their high concentrations (Fritz, 1994).

The majority of cations in the study area (Figure 3) indicated that the concentrations of calcium, magnesium, potassium, aluminum, iron and manganese ions in the Asana River and Altarani Creek were higher in the wet season than in the dry season. This result is because, due to the effects of runoff, the cations are dragged or solubilized from the soil material (Silas, Wuana, & Augustine, 2018); in the case of sodium for the P-11 station, there was a dilution of the cation, which suggests that the source of sodium in this area is underground in nature, and a similar situation occurred at AS-04 (Cardona & Hernández, 2005). However, the concentrations of calcium, magnesium, sodium, potassium, aluminum, iron and manganese cations were higher in Millune Creek in the dry season, which presented different values for aluminum ions (9.5-10.7 mg/l) and manganese (0.348-0.352 mg/l) compared to the values of aluminum (0.034-1.543 mg/l) and manganese (0.004-0.075 mg/l) found in the Asana and Altarani Rivers. Manganese and aluminum oxides are the most reactive components in acidic soils. They release cations by acid weathering of mineral soils, which are reprecipitated as hydrated oxides locally or after translocation, and these precipitates can be quickly

2023, Instituto Mexicano de Tecnología del Agua. Open Access bajo la licencia CC BY-NC-SA 4.0 (https://creativecommons.org/licenses/by-nc-sa/4.0/)

remobilized, producing high concentrations of these ions in water (Paterson, Goodman, & Farmer, 1991), similar to the situation in Millune Creek. The major anions of the study area (Figure 4) indicated that the concentration of bicarbonate ions in the Asana River and Altarani Creek was between 15 and 22.4 mg HCO 3/L; additionally, due to the low values of pH in Millune Creek, the concentration of bicarbonates was lower than the detectable value <0.1 mg HCO 3/L, with dissolved carbon dioxide being the main form of carbon (Vega & Mustain, 2010). The concentration of sulfate ions was higher in Millune Creek (159.8-171.3 mg/l) than in the Asana River and Altarani River (5.1-51.8 mg/l) to the dissolution of sulfated minerals such as alunite (Carrino *et al*., 2015). Additionally, the concentration of sulfates was higher in the dry season in Millune Creek, unlike the Asana and Altarani Rivers, where it was higher in the wet season, which was due to the entry of groundwater and the erosion of new soils from volcanic snow caused by increased thawing in the dry season (Grab, Linde, & De-Lemos, 2016).

2023, Instituto Mexicano de Tecnología del Agua. Open Access bajo la licencia CC BY-NC-SA 4.0 (https://creativecommons.org/licenses/by-nc-sa/4.0/)

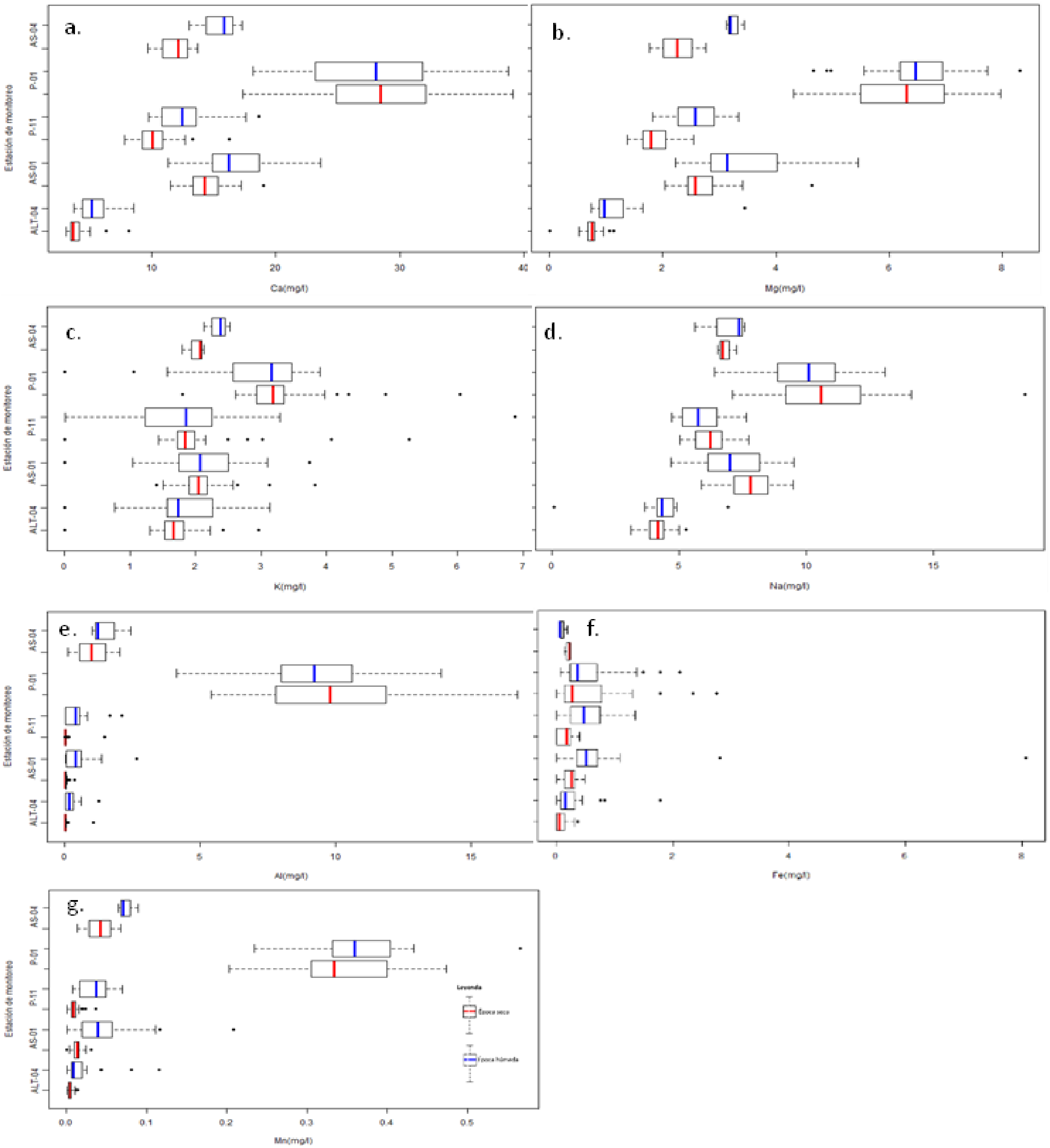

Figure 3. Boxplot diagram of the major cations in the wet and dry seasons: calcium (a), magnesium (b), potassium (c), sodium (d), aluminum (e), iron (f), and manganese (g) in the water from the Asana River, Altarani Creek and Millune Creek.

2023, Instituto Mexicano de Tecnología del Agua. Open Access bajo la licencia CC BY-NC-SA 4.0 (https://creativecommons.org/licenses/by-nc-sa/4.0/)

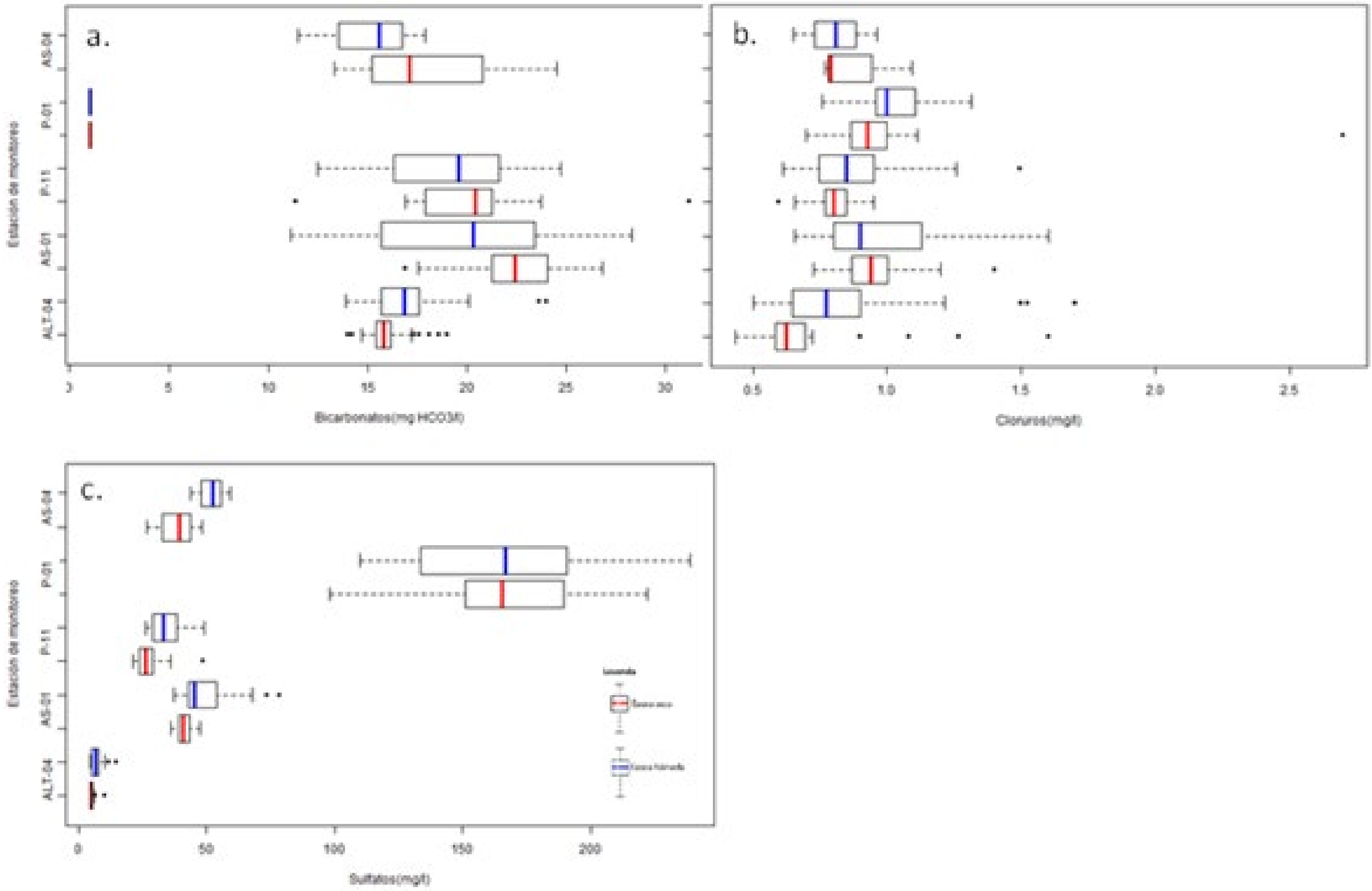

Figure 4. Boxplot diagram of the major anions in the wet and dry seasons: bicarbonates (a), chlorides (b), and sulfates (c) in the water of the Asana River, Altarani Creek and Millune Creek.

Mechanisms that control hydrochemistry

The Piper diagram (Figure 5) shows that the hydrochemistry of the waters of the study area was categorized into two well-defined groups: the water in the Altarani Creek at the ALT-04 station presented a classification of calcium bicarbonate waters, Ca-HCO $_3$, while the waters of the Asana

2023, Instituto Mexicano de Tecnología del Agua. Open Access bajo la licencia CC BY-NC-SA 4.0 (https://creativecommons.org/licenses/by-nc-sa/4.0/)

River (AS-01, P-11 and AS-04) and Millune Creek (P-1) presented calcium sulfated waters, Ca-SO $_4$. The influence of the alkaline waters of Altarani Creek neutralized the acidity of the Asana River at station AS-01, and the influence of the acidic waters of Millune Creek (P-1) was neutralized by the buffer capacity of the Asana River at station AS-04.

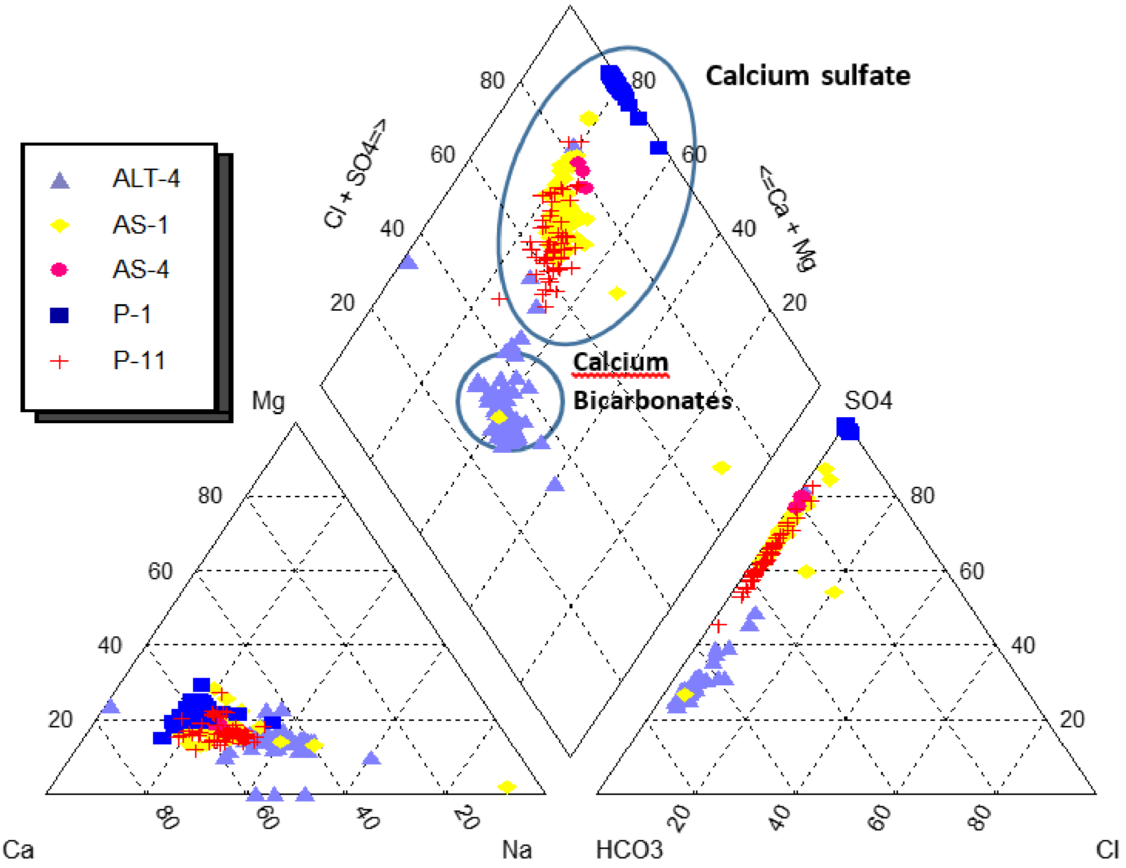

Figure 5. Piper diagram of the waters of the Asana River and Millune Creek.

2023, Instituto Mexicano de Tecnología del Agua. Open Access bajo la licencia CC BY-NC-SA 4.0 (https://creativecommons.org/licenses/by-nc-sa/4.0/)

The water samples from stations ALT-04, AS-01, P-11, P-1 and AS-04 were characterized by moderate concentrations of total dissolved solids (TDS) and low values of Na $+/(Na^{+} + Ca^{2+})$ and $Cl^{-}/(Cl^{-} + HCO_{3}^{-})$, which indicate that the water is dominated by rock weathering products, especially in Millune Creek (P-1), as observed in the Gibbs diagram (Gibbs, 1970) (Figure 6).

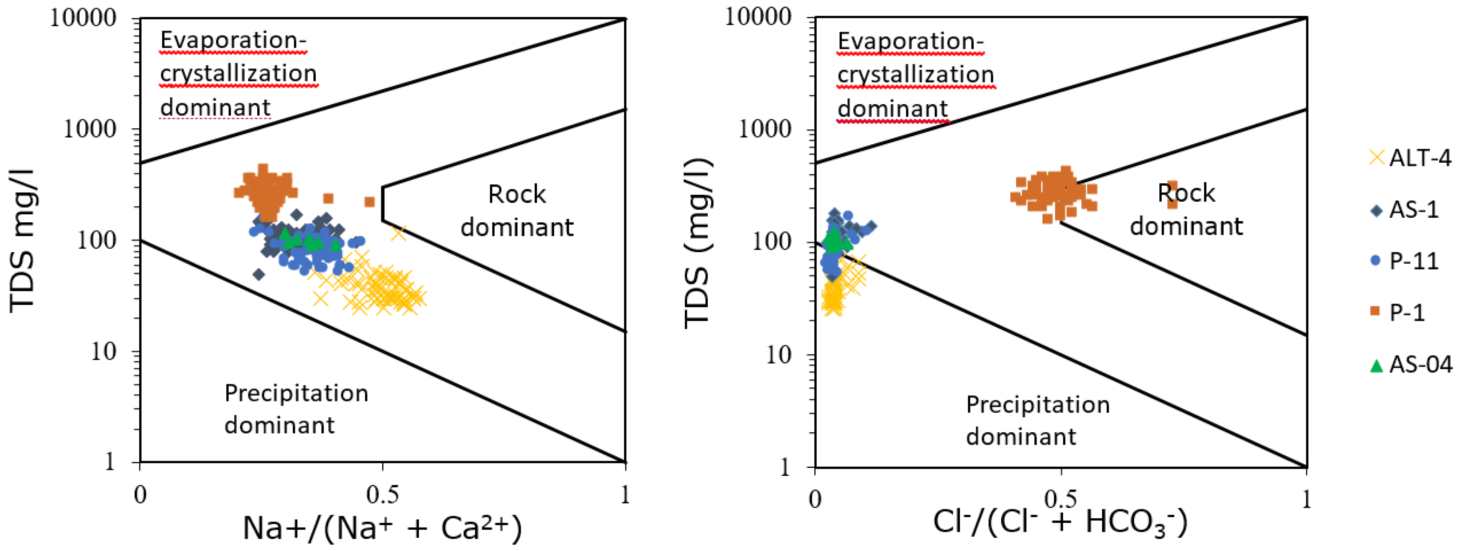

Figure 6. Water chemistry of Millune Creek and the Asana River plotted in the Gibbs diagram. (a) Cation ratio (b) Anion ratio.

In the diagram of the molar ratios of Mg^{2+}/Na^{+} *vs*. Mg^{2+}/Ca^{2+} (Figure 7), it was verified that in Millune Creek (P-1), the rock interactions

2023, Instituto Mexicano de Tecnología del Agua. Open Access bajo la licencia CC BY-NC-SA 4.0 (https://creativecommons.org/licenses/by-nc-sa/4.0/)

regulated the characteristics of the water chemistry due to the effect of the erosion of the new soil product from the thawing of the upstream glacier and bank erosion. In the Asana River (AS-01, P-11 and AS-04) and Altarani Creek (ALT-04), the dissolution of soluble salts in the soil (leaching) was the predominant process.

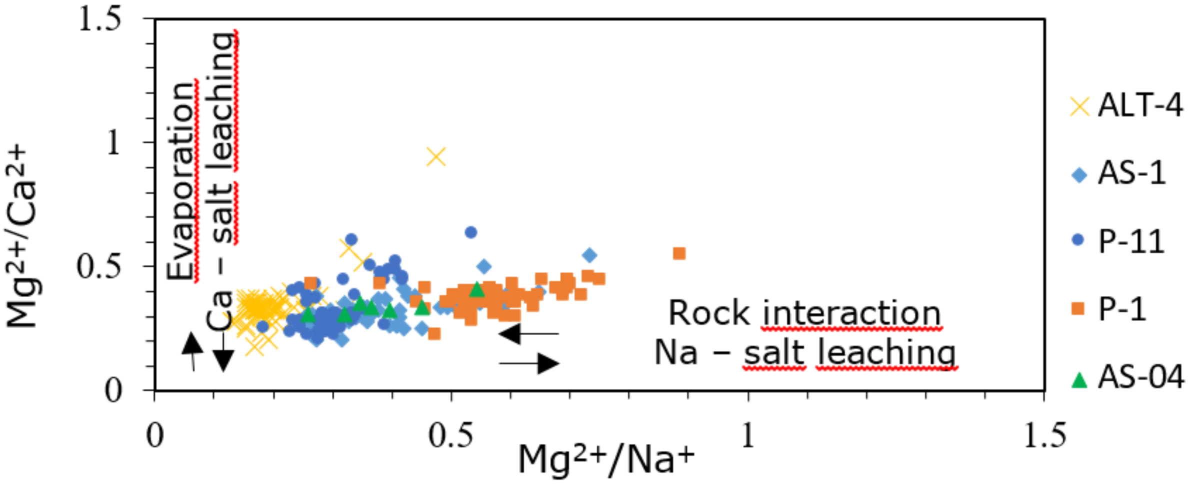

Figure 7. Diagram of the molar ratios of Mg 2+/Ca $^{2+}$ *vs*. Mg $^{2+/Na+}$.

The bivariate diagram of Mg $^{2+}$/Na $^{+}$ *vs*. Ca $^{2+}$/Na $^{+}$ and HCO $_{3}$ $^{-}$/Na $^{+}$ *vs*. Ca $^{2+}$/Na^{+}- (Figure 8) shows that stations ALT-04, AS-01, P-11, P-1 and AS-04 were mainly dominated by silicate weathering, and a low ratio of HCO $_{3}$ $^{-}$/Na $^{+}$ was observed because the bicarbonates were consumed by the acidity generated by the dissolution of sulfated minerals, confirming the presence of aluminosilicate and sulfated minerals such as alumite (KAl $_{3}$ (SO $_{4}$) $_{2}$ (OH) $_{6}$).

2023, Instituto Mexicano de Tecnología del Agua. Open Access bajo la licencia CC BY-NC-SA 4.0 (https://creativecommons.org/licenses/by-nc-sa/4.0/)

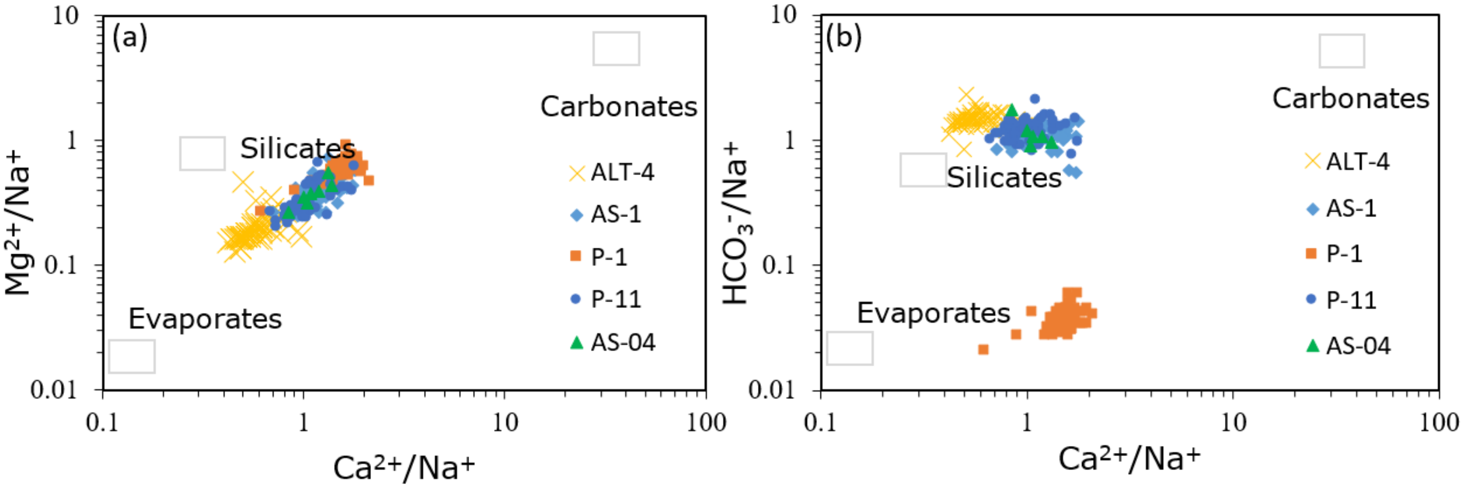

Figure 8. Bivariate diagram of the molar ratios of (a) Mg 2+/Na $^{2+}$ *vs*. Ca 2+/Na $^{+}$ and (b) HCO $_{3}^{-}$/Na $^{+}$ *vs*. Ca 2+/Na $^{+}$.

The results of the hydrochemical modeling in PHREEQC (Figure 9) for the most common minerals in the water of the evaluated monitoring stations showed that the saturation index values followed the trend: biotite> kaolinite> alunite > jarosite> gibsite> aragonite> anhydrite> manganite (Carrino *et al*., 2015). The minerals biotite, kaolinite, alunite, jarosite, and gibsite were supersaturated and generally precipitated at stations ALT-04, AS-01, P-11 and AS-04. However, the saturation index decreased at station P-1 due to the low pH value, which promoted the dissolution of aluminum and sulfates. Additionally, minerals such as anhydrite and manganite were not saturated, so they were dissolved,

2023, Instituto Mexicano de Tecnología del Agua. Open Access bajo la licencia CC BY-NC-SA 4.0 (https://creativecommons.org/licenses/by-nc-sa/4.0/)

increasing the concentrations of sulfates and manganese (Gao *et al*., 2017) at the monitoring stations.

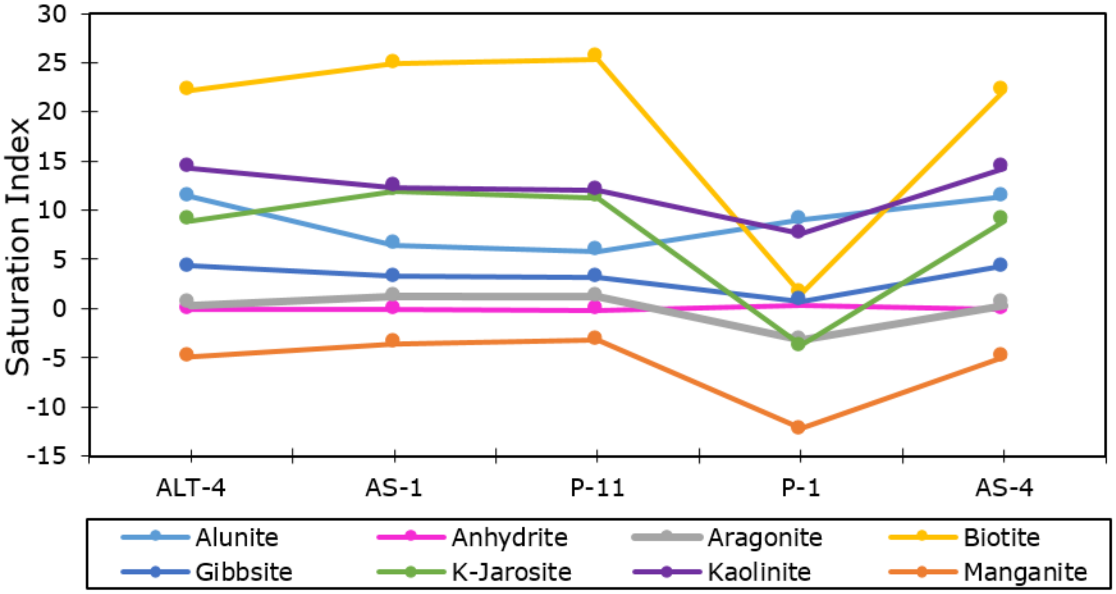

Figure 9. Saturation index (SI) for common minerals at the confluence of Millune Creek and the Asana River.

Landslide susceptibility

The confluence area of Millune Creek and the Asana River were highly susceptible to landslide (Villacorta *et al*., 2012) (Figure 10) due to high weathering, as well as the presence of surface deposits and high slopes; this result indicates that the area is very prone to erosion processes. In this sense, it was confirmed that there was soil erosion caused by the

2023, Instituto Mexicano de Tecnología del Agua. Open Access bajo la licencia CC BY-NC-SA 4.0 (https://creativecommons.org/licenses/by-nc-sa/4.0/)

accelerated thawing of the Arundani glacier (GRM, 2011; ANA, 2018), which then affects Millune Creek, and could be a reason why the reactions in the basin dominated the chemical composition of surface waters.

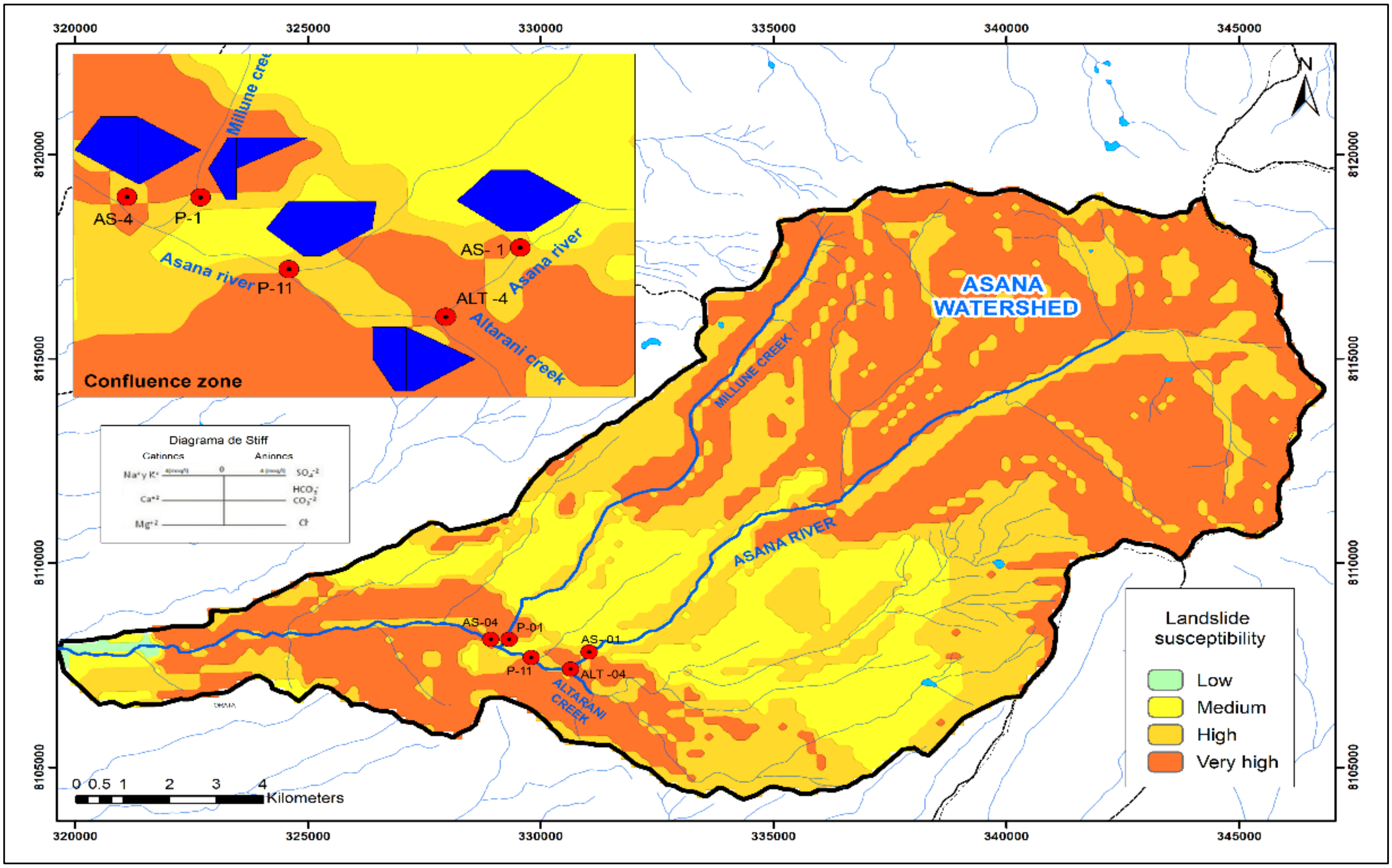

Figure 10. Landslide susceptibility map, confluence of the Millune ravine with the Asana River.

2023, Instituto Mexicano de Tecnología del Agua. Open Access bajo la licencia CC BY-NC-SA 4.0 (https://creativecommons.org/licenses/by-nc-sa/4.0/)

Principal component analysis

Table 1 shows the correlations between the main factors associated with the spatiotemporal variability of water quality in the rivers evaluated; in Altarani Creek (ALT-04), Factor 1 was positively correlated with the flow, total hardness, total dissolved solids, chlorides, sulfates, aluminum, calcium, iron, magnesium and manganese, which was due to the influence of rain on the runoff that transferred the anions and cations by dissolution from the soil material or landslides to the river (Silas *et al*., 2018). Factor 2 was correlated with potassium and nitrate, probably due to anthropogenic activities and the dissolution of silicate material such as biotite. Factor 3 was positively correlated with the increase in electrical conductivity caused by evaporation and the dissolution of metals with the decrease in pH in the dry season (Saarinen & Kløve, 2012). In the Asana River, at stations AS-01 and P-11, Factor 1 was positively correlated with the flow, total hardness, sulfates, aluminum, calcium, iron, magnesium, manganese, and strontium because in the wet season, the effect of rain on runoff dissolves metals and sulfates in soil material or cause soil detachment into water. Factor 2 was negatively correlated with flow, which indicated differentiated behavior in the dry season in the case of AS-01, which was correlated with bicarbonate and sodium by the influence of groundwater, and in the case of P-11, which was correlated with the lower content of aluminum.

2023, Instituto Mexicano de Tecnología del Agua. Open Access bajo la licencia CC BY-NC-SA 4.0 (https://creativecommons.org/licenses/by-nc-sa/4.0/)

Table 1. Analysis by main component of water quality in the study area.

Parameter	ALT-04			AS-01			P-11			P-1			AS-04		
	F1	**F2**	**F3**	**F1**	**F2**	**F3**	**F1**	**F2**	**F3**	**F1**	**F2**	**F3**	**F1**	**F2**	**F3**
Flow	0.66	0.08	-0.33	0.63	-0.53	-0.08	0.50	-0.57	-0.44	-0.47	0.55	-0.07	0.14	0.95	-0.17
OD	-0.01	0.37	0.33	0.15	-0.21	0.52	0.33	-0.01	-0.41	-0.41	0.45	-0.02	0.12	-0.11	0.77
CE	0.04	0.26	0.75	0.141	-0.04	0.68	0.35	0.68	-0.17	0.40	0.18	0.23	0.46	-0.33	-0.74
pH	-0.04	-0.39	-0.65	-0.05	0.36	-0.39	-0.15	-0.28	0.60	-0.41	0.48	0.29	-0.26	0.30	0.68
HCO$_3$	0.30	-0.03	-0.35	-0.68	0.59	0.005	-0.46	-0.23	0.46				-0.59	-0.61	-0.13
Total hardness	0.76	-0.47	0.23	0.78	0.40	-0.02	0.85	0.02	0.36	0.94	0.06	-0.07	0.97	0.19	-0.10
TDS	0.73	-0.31	0.46	0.41	0.29	0.43	0.62	0.52	-0.01	0.70	-0.002	-0.22	0.79	-0.19	-0.09
Cl-	0.64	0.43	-0.08	0.48	0.42	0.15	0.64	0.01	0.21	-0.05	0.02	0.59	-0.77	0.41	-0.35
NO$_3$-N	0.68	0.52	-0.19	0.71	-0.35	0.13	0.71	-0.24	-0.21	-0.43	-0.25	0.54	0.17	0.90	-0.07
SO$_4$	0.79	0.42	-0.13	0.85	0.13	-0.11	0.88	0.22	0.27	0.95	0.10	-0.05	0.92	-0.25	-0.21
Al	0.75	0.13	-0.13	0.78	-0.16	-0.20	0.58	-0.54	-0.12	0.77	0.36	0.11	0.77	-0.38	0.05
Ca	0.76	0.14	-0.09	0.72	0.29	-0.05	0.74	0.20	0.497	0.89	0.002	-0.02	0.93	-0.14	0.19
Fe	0.74	-0.14	-0.14	0.78	0.12	-0.17	0.74	-0.45	0	-0.13	0.68	0.19	-0.49	-0.69	-0.27
Mg	0.81	-0.47	0.11	0.85	0.05	-0.08	0.88	-0.19	0.03	0.85	0.15	0.07	0.94	0.23	-0.01
Mn	0.88	0.13	-0.141	0.89	-0.11	-0.21	0.86	-0.35	0.03	0.88	0.18	-0.02	0.92	0.04	0.05
K	0.34	0.57	0.21	0.41	0.19	0.45	0.37	0.63	-0.34	0.24	-0.04	0.55	0.74	0.65	-0.07
Na	0.43	-0.31	0.26	-0.12	0.85	-0.004	-0.20	0.10	0.49	0.55	-0.31	0.49	0.44	-0.85	0.26
Sr	0.86	-0.42	0.18	0.66	0.29	0.05	0.75	0.38	0.09	0.87	0.02	0.05	0.98	-0.17	0.03
%	40.73	52.98	63.37	38.78	51.83	59.93	39.87	53.9	64.34	42.31	51.64	60.08	49.1	73.83	85.02
🟧	Forts			🟨	Moderates			⬜	Weaks						

In Millune Creek (P-1), Factor 1 was positively correlated with total hardness, total dissolved solids, sulfates, aluminum, calcium, magnesium,

2023, Instituto Mexicano de Tecnología del Agua. Open Access bajo la licencia CC BY-NC-SA 4.0 (https://creativecommons.org/licenses/by-nc-sa/4.0/)

manganese, sodium and strontium because in the dry season, and this correlation was due to the greater oxidation of the sulfated soil material, the low pH values that dissolved the metals from the creek bed, and the effect of the melting of the ice and snowfall that then leach metals from the new soil. Factor 2 was positively correlated with flow and iron because in the wet season, the concentration of metals is diluted by increasing flow; however, the positive correlation with iron indicates that the source of this in the stream is runoff in the wet season (Silas *et al*., 2018). In the Asana River, at the AS-04 station, which is located downstream of the confluence with Millune Creek, Factor 1 was positively correlated with hardness, total dissolved solids, sulfates, aluminum, calcium, magnesium, manganese, potassium and strontium. This correlation was independent of flow. Factor 2 was positively correlated with the flow, nitrates and potassium, which was probably related to anthropogenic activities. There was also a negative correlation with bicarbonates, iron and sodium, which indicated that in the rainy season, their concentration decreased due to dilution. Factor 3 was positively correlated with dissolved oxygen and pH and negatively correlated with conductivity because the increase in pH reduced the dissolution of metals in the soil, thus decreasing the conductivity and the increase in dissolved oxygen when the pH decreased; this process was related to photosynthetic processes.

Liu*,* Lin and Kuo (2003) classified the correlations as "strong", "moderate" and "weak", which corresponded to the absolute value of the loads greater than 0.75, between 0.75-0.50 and between 0.50-0.30, respectively.

2023, Instituto Mexicano de Tecnología del Agua. Open Access bajo la licencia CC BY-NC-SA 4.0 (https://creativecommons.org/licenses/by-nc-sa/4.0/)

Conclusions

The hydrochemistry of the Asana River and Millune Creek was characterized by calcium sulfated waters; however, the latter presented low pH values and high concentrations of aluminum, manganese and sulfates and was dominated by the processes of weathering of rocks with alumino-sulfated minerals such as alunite, increasing the concentration of aluminum and manganese ions in the Asana River at the confluence. The buffer capacity of the Asana River reduced the dissolution of metals and favored the alkalinity of the waters of Altarani Creek; in addition, it neutralized the low pH values of Millune Creek.

The melting of the snow-capped mountains as a result of climate change reveals erodible soils that contribute minerals to the channel of Millune Creek, which is one reason why the reactions in the hydrographic basin are the main control mechanism responsible for the hydrochemical variability in Millune Creek. The latter flowing into the Asana River influences its hydrochemical composition.

The results provide a scientific basis on the hydrochemical variability and environmental changes in the Asana basin, and these results can be useful in the management and decision-making regarding the study area, which will allow a better understanding of the hydrochemical dynamics and mechanisms that control it. This information can be used to evaluate adaptation measures, identify water treatment alternatives and identify areas with potential natural contamination.

2023, Instituto Mexicano de Tecnología del Agua. Open Access bajo la licencia CC BY-NC-SA 4.0 (https://creativecommons.org/licenses/by-nc-sa/4.0/)

Acknowledgments

To the Center of Research in Chemistry, Toxicology and Environmental Biotechnology of the Universidad Nacional Agraria La Molina (CIQTOBIA-UNALM) for their advice in the discussion of the results obtained in the research. The comments and suggestions of the anonymous reviewers that allowed the improvement of the article are appreciated.

References

Acero, P., Hudson-Edwards, K. A., & Gale, J. D. (2015). Influence of pH and temperature on alunite dissolution: Rates, products and insights on mechanisms from atomistic simulation. *Chemical Geology*, 419, 1-9. DOI: 10.1016/j.chemgeo.2015.10.018

ANA, Autoridad Nacional del Agua del Perú. (2018). *Clasificación de los cuerpos de agua continentales superficiales, Lima, Perú*. Recovered from https://hdl.handle.net/20.500.12543/2439

Ban, Y., Lei, T., Chen, C., & Liu, Z. (2016). Study on the facilities and procedures for meltwater erosion of thawed soil. *International Soil and Water Conservation Research*, 4(2), 142-147. DOI: 10.1016/j.iswcr.2016.04.003

Cardona, A., & Hernández, N. (1995). Modelo geoquímico conceptual de la evolución del agua subterránea en el valle de México. *Ingeniería Hidráulica en México*, 10(3), 71-90.

2023, Instituto Mexicano de Tecnología del Agua. Open Access bajo la licencia CC BY-NC-SA 4.0 (https://creativecommons.org/licenses/by-nc-sa/4.0/)

Carrino, T. A., Crosta, A. P., Toledo, C. L. B., Silva, A. M., & Silva, J. L. (2015). Geology and hydrothermal alteration of the Chapi Chiara prospect and nearby targets, southern Peru, using ASTER data and reflectance spectroscopy. *Economic Geology*, 110(1), 73-90. DOI: 10.2113/econgeo.110.1.73

De-Andrade, E. M., Palácio, H. A. Q., Souza, I. H., De-Oliveira-Leão, R. A., & Guerreiro, M. J. (2008). Land use effects in groundwater composition of an alluvial aquifer (Trussu River, Brazil) by multivariate techniques. *Environmental Research*, 106(2), 170-177. DOI: 10.1016/j.envres.2007.10.008

Devic, G., Djordjevic, D., & Sakan, S. (2014). Natural and anthropogenic factors affecting the groundwater quality in Serbia. *Science of the Total Environment*, 468-469, 933-942. DOI: 10.1016/j.scitotenv.2013.09.011

Ece, Ö. I., Schroeder, P. A., Smilley, M. J., & Wampler, J. M. (2008). Acid-sulphate hydrothermal alteration of andesitic tuffs and genesis of halloysite and alunite deposits in the Biga Peninsula, Turkey. *Clay Minerals*, 43(02), 281-315. doi:10.1180/claymin.2008.043.2.10

El-Alfy, M., Aref, L., Fathy, A., & Abdulaziz, A.-B. (2017). Assessing the hydrogeochemical processes affecting groundwater pollution in arid areas using an integration of geochemical equilibrium and multivariate statistical techniques. *Environmental Pollution*, 229(2017), 760-770. DOI: 10.1016/j.envpol.2017.05.052

2023, Instituto Mexicano de Tecnología del Agua. Open Access bajo la licencia CC BY-NC-SA 4.0 (https://creativecommons.org/licenses/by-nc-sa/4.0/)

Fritz, S. J. (1994). A survey of charge-balance errors on published analyses of potable ground and surface waters. *Ground Water*, 32(4), 539-546. doi:10.1111/j.1745-6584.1994.tb00888.x

Gao, Z., Lin, Z., Niu, F., Luo, J., Liu, M., & Yin, G. (2017). Hydrochemistry and controlling mechanism of lakes in permafrost regions along the Qinghai-Tibet Engineering Corridor, China. *Geomorphology*, 297, 159–169. doi: 10.1016/j.geomorph.2017.09.020

Gibbs, R. J. (1970). Mechanisms controlling world water chemistry. *Science*, 170(3962), 1088-1090. DOI: 10.1126/science.170.3962.1088

Grab, S., Linde, J., & De Lemos, H. (2017). Some attributes of snow occurrence and snowmelt/sublimation rates in the Lesotho Highlands: environmental implications. *Water SA*, 43(2), 333-342.

GRM, Gobierno Regional de Moquegua. (2011). *Estudio de diagnóstico y zonificación para fines de demarcación territorial de la provincia Mariscal Nieto*. Moquegua, Perú: Gobierno Regional de Moquegua.

Hamzah, Z., Aris, A. Z., Ramli, M. F., Juahir, H., & Sheikhy-Narany, T. (2017). Groundwater quality assessment using integrated geochemical methods, multivariate statistical analysis, and geostatistical technique in shallow coastal aquifer of Terengganu, Malaysia. *Arabian Journal of Geosciences*, 10(2). DOI: 10.1007/s12517-016-2828-5

Han, G., & Liu, C. (2000). Hydrogeochemistry of Wujiang River water in GuiZhou province. *Carsologica Sinica*, 19, 35-43.

2023, Instituto Mexicano de Tecnología del Agua. Open Access bajo la licencia CC BY-NC-SA 4.0 (https://creativecommons.org/licenses/by-nc-sa/4.0/)

Helena, B., Pardo, R., Veja, M., Barrado, E., Fernandez, J. M., & Fernandez, L. (2000). Temporal evolution of groundwater composition in an alluvial aquifer (Pisuerga River, Spain) by principal component analysis. *Water Research*, 34(3), 807-816. DOI: 10.1016/s0043-1354(99)00225-0

Jiang, J., Tang, S., Han, D., Fu, G., Solomatine, D., & Zheng, Y. (2020). A comprehensive review on the design and optimization of surface water quality monitoring networks*. Environmental Modelling & Software*, 104792. DOI: 10.1016/j.envsoft.2020.104792

Knight Piésold Consultores, S. A. (2008). *Modificación del estudio de impacto ambiental – Proyecto Quellaveco*. Recovered from http://www.minem.gob.pe/minem/archivos/file/DGAAM/ estudios/ quellaveco/1.%20Texto.pdf

Liu, C. W., Lin, K. H., & Kuo, Y. M. (2003). Application of factor analysis in the assessment of groundwater quality in a blackfoot disease area in Taiwan. Science of the total environment, 313(1-3), 77-89.

Luque-Poma, G., Pari-Pinto, W., Dueñas-Olivera, K. L., Huamán-Nieto, M. (2020). Peligro geológico en la región. *Boletín Ingemmet. Serie C: Geodinámica e Ingeniería Geológica*, 75, 252. Recovered from https://hdl.handle.net/20.500.12544/2565

Montesinos, D. B., Cleef, A. M., & Sykora, K. V. (2012). Andean shrublands of Moquegua, South Peru: Prepuna plant communities. *Phytocoenologia*, 42(1-2), 29-55. DOI: 10.1127/0340-269x/2012/0042-0516

2023, Instituto Mexicano de Tecnología del Agua. Open Access bajo la licencia CC BY-NC-SA 4.0 (https://creativecommons.org/licenses/by-nc-sa/4.0/)

Ng, W., Peña, N., & Acosta, H. (2019). Hidrogeología de la cuenca del río Ilo- Moquegua, Región Moquegua, INGEMMET. *Boletín Ingemmet. Serie H: Hidrogeología*, 6, 292.

Ouyang, Y. (2005). Evaluation of river water quality monitoring stations by principal component analysis. *Water Research*, 39(12), 2621-2635. DOI: 10.1016/j.watres.2005.04.024

Parkhurst, D. L., & Appelo, C. A. J. (1999). User's guide to PHREEQC (Version 2) – A computer program for speciation, batch-reaction, one-dimensional transport, and inverse geochemical calculations. *U.S. Geological Survey*, 99-4259. Recovered from https://doi.org/10.3133/wri994259

Paterson, E., Goodman, B. A., & Farmer, V. C. (1991). The chemistry of aluminium, iron and manganese oxides in acid soils. *Soil Acidity*, 97-124. DOI: 10.1007/978-3-642-74442-6_5

Qin, K., Liu, J., Yan, L., & Huang, H. (2019). Integrating ecosystem services flows into water security simulations in water scarce areas: Present and future. *Science of the Total Environment*, 670, 1037-1048. DOI: 10.1016/j.scitotenv.2019.03.263

Rau, P. (2017). *Precipitation runoff and water balance regimes variability along the Peruvian Pacific slope and coast: ENSO influence and sensivity to hydroclimatic change* (tesis doctoral). Université Paul Sabatier-Toulouse III, ffNNT: 2017TOU30249ff, fftel-01925488ff

2023, Instituto Mexicano de Tecnología del Agua. Open Access bajo la licencia CC BY-NC-SA 4.0 (https://creativecommons.org/licenses/by-nc-sa/4.0/)

Saarinen, T. S., & Kløve, B. (2012). Past and future seasonal variation in pH and metal concentrations in runoff from river basins on acid sulphate soils in Western Finland. *Journal of Environmental Science and Health*, Part A, 47(11), 1614-1625. DOI: 10.1080/10934529.2012.680783

Schreier, H., Erlebach, W., & Albright, L. (1980). Variations in water quality during winter in two Yukon rivers with emphasis on dissolved oxygen concentration. *Water Research*, 14(9), 1345-1351. DOI: 10.1016/0043-1354(80)90195-5

Silas, I., Wuana, R. A., & Augustine, A. U. (2018). Seasonal variation in water quality parameters of river Mkomon Kwande local goverment Area, Nigeria. *International Journal of Recent in Physics and Chemical Sciences*, 5(1), 42-62.

Stiff, H. A. (1951). The interpretation of chemical water analysis by means of patterns. *Journal of Petroleum Technology*, 3(10), 15-17. Recovered from https://doi.org/10.2118/951376-G

Thomas, J., Joseph, S., & Thrivikramji, K. P. (2015). Hydrochemical variations of a tropical mountain river system in a rain shadow region of the southern Western Ghats, Kerala, India. *Applied Geochemistry*, 63, 456-471.

Vega, J, A., & Mustain, W. E. (2010). Effect of CO2, HCO3− and CO3−2 on oxygen reduction in anion exchange membrane fuel cells. *Electrochimica Acta*, 55(5), 1638-1644. DOI: 10.1016/j.electacta.2009.10.041

2023, Instituto Mexicano de Tecnología del Agua. Open Access bajo la licencia CC BY-NC-SA 4.0 (https://creativecommons.org/licenses/by-nc-sa/4.0/)

Vörösmarty, C. J., McIntyre, P. B., Gessner, M. O., Dudgeon, D., Prusevich, A., Green, P., Davies, P. M. (2010). Global threats to human water security and river biodiversity. *Nature*, 467(7315), 555-561. DOI: 10.1038/nature09440

Villena-Chávez, J. A. (2018). Calidad del agua y desarrollo sostenible. *Revista Peruana de Medicina Experimental y Salud Pública*, 35(2), 304. Recovered from https://doi.org/10.17843/rpmesp.2018.352.3719

Villacorta, S., Fidel, L., & Zavala, B. (2012). Mapa de susceptibilidad por movimientos en masa del Perú. *Revista de la Asociación Geológica Argentina*, 69(3), 393-399.

Waterloo Hydrogeologic. (2020). *User's Manual AquaChem 9.0, Water Quality Analysis Software*. Waterloo, Canada: Waterloo Hydrogeologic.

2023, Instituto Mexicano de Tecnología del Agua. Open Access bajo la licencia CC BY-NC-SA 4.0 (https://creativecommons.org/licenses/by-nc-sa/4.0/)